Int. J. Solids Structures Vol. 29, No. 1, pp. 1–25, 1992
Printed in Great Britain.

0020–7683/92 $3.00+.00

INFLUENCE OF DISTRIBUTED AND LOCALIZED IMPERFECTIONS ON THE BUCKLING OF CYLINDRICAL SHELLS UNDER EXTERNAL PRESSURE

R. ABDELMOULA
EDF, Clamart, France

N. DAMIL
Université Hassan II, Faculté des Sciences II, Ben M'Sik, Casablanca, Morocco

and

M. POTIER-FERRY
Laboratoire de Physique et Mécanique des Matériaux, Unité de Recherche Associée au CNRS 1215, Faculté des Sciences, Ile du Saulcy, 57045 Metz, France

(*Received* 29 *May* 1990; *in revised form* 2 *March* 1991)

Abstract—The influence of distributed and/or localized imperfections on the buckling load is analysed within the framework of cellular bifurcation theory. We propose analytical formulae for the reduction of the critical buckling pressure of those shells in the presence of various types of imperfections.

1. INTRODUCTION

The buckling analysis of thin cylindrical shells gave rise to a number of studies. These structures are frequently used in aeronautics and in mechanical, nuclear and civil engineering. Several recent books are devoted to theoretical, numerical and experimental developments about perfect and imperfect thin cylindrical shells (Yamaki, 1984; Bushnell, 1985; Arbocz *et al.*, 1987; Dubas and Van De Pite, 1987; Hui *et al.*, 1989).

The most important feature of curved shells is their high imperfection sensitivity. In this paper, we propose closed form formulae to predict buckling of cylindrical shells under external pressure in the presence of various types of imperfections.

The classical post-buckling theory (Koiter, 1945; Thompson and Hunt, 1973; Budiansky, 1974; Potier-Ferry, 1987) can be used for imperfect structures if the number of buckling modes is finite. Using the Lyapounov–Schmidt method, these theories lead to algebraic amplitude equations. In the case of a single buckling mode of an unstable bifurcation and in the presence of an imperfection of amplitude a_0, one gets a reduction of the critical load which is proportional to $a_0^{2/3}$.

For pressurized thin cylindrical shells the buckled states have a cellular shape in the circumferential direction, with a rather large azimuthal wavenumber n. Thus many buckling modes are nearly coincident and their non-linear interaction must be accounted for in an imperfection sensitivity analysis. This interaction between different wavenumbers can lead to spatial variation of the amplitude of the post-buckling pattern, which is modelled by a complex differential equation. This equation is nowadays referred to as the Ginzburg–Landau equation. It was first obtained in the study of convective rolls (Segel, 1969; Newell and Whitehead, 1969). The effect of localized imperfections on the buckling load can be analysed by using the Ginzburg–Landau equation (Amazigo *et al.*, 1970; Amazigo and Frazer, 1971; Damil and Potier-Ferry, 1991). In their study of a beam buckling problem, Amazigo *et al.* (1970) established that the amplitude of the buckling pattern has a discontinuous derivative in the region where the localized imperfection is significant. This leads to a reduction of the critical load proportional to the amplitude a_l of the localized imperfection.

In a previous paper (Damil and Potier-Ferry, 1991) we established that any cellular instability problem is governed by amplitude equations of the Ginzburg–Landau type. We also showed how to account for distributed and/or localized imperfections. In particular, we have extended to any cellular instability problem the localized imperfection analysis due to Amazigo *et al.* (1970). Moreover, the coefficients of these equations and the corresponding discontinuities are obtained in closed form, which permits their analytical computation.

This method will be used in this paper to calculate the maximal pressure of circular cylindrical shells which have a large geometrical Batdorf parameter Z in the presence of distributed and/or localized imperfections.

In order to get closed form formulae for the reduction of critical pressure, we shall use an additional approximation. Indeed, the buckling modes of cylinders under external pressure are nearly inextensional and are more rapidly varying in the circumferential direction than in the axial direction. From these facts Abdelmoula and Potier-Ferry (1991) established an approximate buckling analysis that is valid for sufficiently large values of the Batdorf parameter. The present non-linear analysis will be carried out within this approximation.

2. DONNELL EQUATIONS AND INEXTENSIONAL APPROXIMATION

We consider a circular cylindrical shell of radius R, length L and thickness h, which is made of a homogeneous, isotropic elastic material with Young's modulus E and Poisson's ratio ν. It is subjected to an external normal pressure P. The coordinate system is taken as shown in Fig. 1 and the displacement components will be denoted by u, v and w.

Within Donnell theory and if the pre-buckling rotations are neglected, in the presence of an initial displacement $d(x, y)$, the transverse displacement $w(x, y)$ and the additional stress function $f(x, y)$ are solutions of

$$\begin{cases} D\Delta^2 w - \dfrac{1}{R}\partial_x^2 f + PR\left(\dfrac{\alpha}{2}\partial_x^2 w + \partial_y^2 w\right) - [w, f] + PR\left(\dfrac{\alpha}{2}\partial_x^2 d + \partial_y^2 d\right) - [d, f] = 0 \\ \dfrac{1}{Eh}\Delta^2 f + \dfrac{1}{R}\partial_x^2 w = -\tfrac{1}{2}[w, w] - [w, d] \end{cases} \tag{1}$$

where α is equal to 1 or 0 depending on the application of P on the whole of the boundary or only on the lateral part. We use the following notation:

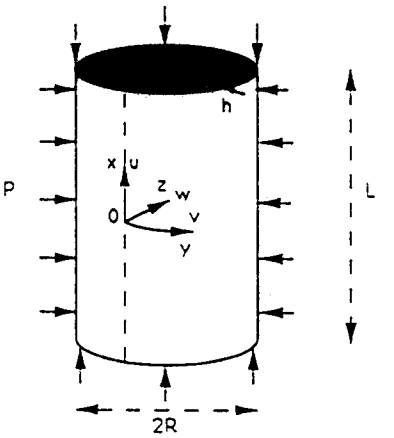

Fig. 1. Cylinder subjected to uniform external pressure.

$$\partial_x = \frac{\partial}{\partial x} \quad \partial_y = \frac{\partial}{\partial y} \quad \Delta^2 = (\partial_x^2 + \partial_y^2)^2$$

$$[g,h] = (\partial_x^2 g)(\partial_y^2 h) + (\partial_y^2 g)(\partial_x^2 h) - 2(\partial_{xy}^2 g)(\partial_{xy}^2 h) \quad D = \frac{Eh^3}{12(1-\nu^2)}.$$

The stress function f is related to the resultant stress by

$$N_x = \partial_y^2 f, \quad N_y = \partial_x^2 f, \quad N_{xy} = -\partial_{xy}^2 f.$$

Different boundary conditions at $x = -L/2$ and $x = L/2$ are considered (C is clamped and S is simply supported):

$$\begin{aligned}
&\text{C1}: w = \partial_x w = u = v = 0 && \text{S1}: w = \partial_x^2 w = u = v = 0\\
&\text{C2}: w = \partial_x w = u = N_{xy} = 0 && \text{S2}: w = \partial_x^2 w = u = N_{xy} = 0\\
&\text{C3}: w = \partial_x w = N_x = v = 0 && \text{S3}: w = \partial_x^2 w = N_x = v = 0\\
&\text{C4}: w = \partial_x w = N_x = N_{xy} = 0 && \text{S4}: w = \partial_x^2 w = N_x = N_{xy} = 0.
\end{aligned} \tag{2}$$

The buckling mode of the pressurized cylindrical shell satisfies the linearized equations

$$\begin{cases} D\Delta^2 w - \dfrac{1}{R}\partial_x^2 f + PR\left(\dfrac{\alpha}{2}\partial_x^2 w + \partial_y^2 w\right) = 0 \\ \dfrac{1}{Eh}\Delta^2 f + \dfrac{1}{R}\partial_x^2 w = 0. \end{cases} \tag{3}$$

The classical harmonic solutions of eqn (3) have a slower variation in the axial direction than in the circumferential direction for large geometrical Batdorf parameter $Z = \sqrt{1-\nu^2}L^2/Rh$ ($Z \geqslant 500$). These buckling modes have a large circumferential wavenumber and are nearly inextensional, that is, the membrane buckling strain is weak. From these facts, Abdelmoula and Potier-Ferry (1991) established an approximate buckling analysis. This leads to neglect of $\partial/\partial x$ with respect to $\partial/\partial y$, except in the coupling terms $\partial_x^2 f$ and $\partial_x^2 w$. Thus the mode and the buckling pressure can be approximated by the solutions of:

$$\begin{cases} D\partial_y^4 w - \dfrac{1}{R}\partial_x^2 f + PR\partial_y^2 w = 0 \\ \dfrac{1}{Eh}\partial_y^4 f + \dfrac{1}{R}\partial_x^2 w = 0. \end{cases} \tag{4}$$

This implies a loss of two boundary conditions and the existence of boundary layers. Within this approximate analysis, it has been established that the boundary conditions for the approximate system (4) can be stated as follows, according to the boundary conditions (2) of the exact system:

1. If there is no axial restraint ($N_x = 0$)

$$w\left(\pm\frac{L}{2}, y\right) = 0 \quad \text{and} \quad f\left(\pm\frac{L}{2}, y\right) = 0. \tag{5}$$

2. If there is an axial restraint ($u = 0$)

$$w\left(\pm\frac{L}{2}, y\right) = 0 \quad \text{and} \quad \partial_x w\left(\pm\frac{L}{2}, y\right) = 0. \tag{6}$$

In the present non-linear analysis, this approximation will be used in order to get closed form formulae for the reduction of critical pressure in the presence of imperfections. We also neglect $\partial/\partial x$ with respect to $\partial/\partial y$ in the non-linear equations (1). The post-buckling behaviour is then governed by the approximate equations:

$$\begin{cases} D\partial_y^4 w - \dfrac{1}{R}\partial_x^2 f + PR\partial_y^2 w - [w, f] + PR\partial_y^2 d = 0 \\ \dfrac{1}{Eh}\partial_y^4 f + \dfrac{1}{R}\partial_x^2 w = -\frac{1}{2}[w, w] \end{cases} \tag{7}$$

with the boundary conditions (5) or (6). We have neglected the higher order terms $[d, f]$ and $[d, w]$. The solutions of eqns (7) are extrema of the following Reissner-type functional:

$$\mathscr{L}(P, w, f) = \frac{1}{2}\int_\Omega \left\{D(\partial_y^2 w)^2 - \frac{1}{Eh}(\partial_y^2 f)^2 - \frac{2}{R}\partial_x^2 f w - PR(\partial_y w)^2\right\} dx\, dy - \frac{1}{2}\int_\Omega [w, f] w\, dx\, dy \tag{8}$$

where $\Omega = [-L/2, L/2] \times [0, 2\pi R]$. This functional will be used to compute the imperfection sensitivity factor b.

For the shells considered, the buckling mode has a cellular shape in the circumferential direction. Furthermore, the wavenumber n is rather large provided that the ratio L/R is not too large (otherwise Donnell shell theory would not be valid). Therefore classical bifurcation theory is only relevant to get exactly periodic patterns. So we shall apply cellular bifurcation theory in order to account for non-periodic imperfections and for non-periodic solutions. To fit with the framework of cellular bifurcation theory, let us rewrite the post-buckling problem (7) as follows:

$$\frac{d\mathbf{u}}{dy} = \mathbf{F}(P, \mathbf{u}) + \mathbf{G}(y) \tag{9}$$

where we have put

$$'\{\mathbf{u}\} = \{w, f, \partial_y^2 w, \partial_y^2 f, \partial_y w, \partial_y f, \partial_y^3 w, \partial_y^3 f\}$$
$$= \{s_1, s_2, s_3, s_4, s_5, s_6, s_7, s_8\} \tag{10a}$$

$$'\{\mathbf{F}\} = \left\{s_5, s_6, s_7, s_8, s_3, s_4, \frac{1}{D}\left(\frac{1}{R}\partial_x^2 s_2 - PRs_3 + s_4\partial_x^2 s_1 + s_3\partial_x^2 s_2 - 2\partial_x s_5\partial_x s_6\right),\right.$$
$$\left. Eh\left(-\frac{1}{R}\partial_x^2 s_1 - \partial_x^2 s_1 s_3 + \frac{1}{2}(\partial_x s_5)^2\right)\right\} \tag{10b}$$

$$'\{\mathbf{G}(y)\} = \left\{0, 0, 0, 0, 0, 0, -\frac{PR}{D}\partial_y^2 d(x, y), 0\right\} \tag{10c}$$

where $\mathbf{F}(P, \mathbf{u})$ is a non-linear operator which depends on the axial variable x. The vector $\mathbf{G}(y)$ accounts for initial imperfections, and $'\{\mathbf{u}\}$ denotes the transpose of a column vector.

3. CELLULAR INSTABILITIES

3.1. *Basic features*

In order to apply the classical perturbed bifurcation theory (Koiter, 1945; Thompson and Hunt, 1973; Budiansky, 1974; Potier-Ferry, 1987) it is required that, at the bifurcation load P_c, the number of buckling modes is finite, in which case the Lyapounov–Schmidt method leads to algebraic amplitude equations. In the case of a single buckling mode of an unstable symmetric bifurcation and in the presence of an imperfection of amplitude a_0, the amplitude equation has the following form:

$$(P-P_c)\alpha_{11}a+\alpha_{30}a^3+\beta a_0 = 0. \tag{11}$$

The numerical coefficients α_{11} and α_{30} are related to the perfect structure, the loading and the boundary conditions. Within the classical theory, a simple formula yields the imperfection sensitivity factor $b = -\alpha_{30}/\alpha_{11}$ as a function of the buckling mode and of the potential energy. The coefficient β is somewhat like a projection of the imperfections on the buckling mode. From (11), one finds a maximal load P_m which is lower than P_c, the corresponding reduction of the critical load being proportional to $(a_0)^{2/3}$.

In the case of a cellular bifurcation, the algebraic equation is replaced by a complex differential equation of the Ginzburg–Landau type (here without imperfection):

$$\frac{d^2a}{dy^2}+(P-P_c)\alpha_1 a+\alpha_2 a|a|^2 = 0 \tag{12}$$

which permits one to account for spatial variations of the amplitude of the post-buckling patterns. The coefficients α_1 and α_2 are real and they are to be computed in each problem. The influence of localized imperfections on buckling load can also be studied by this equation, as established by Amazigo *et al.* (1970).

3.2. *General framework*

In a previous paper (Damil and Potier-Ferry, 1991), we established that for any cellular instability problem, the instability pattern is governed by amplitude equations of the Ginzburg–Landau type with new terms that account for imperfections. In this method, the perturbed Ginzburg–Landau equation and the jump condition due to localized imperfections are given by general formulae.

We have considered a general differential equation of the form:

$$\frac{d\mathbf{u}}{dy} = \mathbf{F}(P,\mathbf{u})+a_0\mathbf{G}_0(y)+a_l\mathbf{G}_l(y) \tag{13}$$

where y lies in an interval whose length is large with respect to the wavelength and P is the real control parameter (here the pressure). It is clear that Donnell equations (1) or approximate Donnell equations (7) can be written in this form [see eqn (9)].

In what follows, we distinguish between distributed imperfections and localized imperfections, the latter being significant in a small region of the shell, say one or two buckles. We have denoted the amplitude of the distributed imperfection by a_0, its shape by $\mathbf{G}_0(y)$, the amplitude of the localized imperfection by a_l, and its shape by $\mathbf{G}_l(y)$.

Our general results can be expressed only in terms, first of the factor b of the nonlinear classical bifurcation theory and second of the linear bifurcation problem. A cellular bifurcation occurs when the linear part $L(P)$ of the operator $\mathbf{F}$ has a double but not semi-simple eigenvalue on the imaginary axis. We denote by $\mathbf{U}_c$ and $\mathbf{V}_c$ the corresponding eigenvectors:

$$L(P_c)\mathbf{U}_c = iq_c\mathbf{U}_c$$

$$L(P_c)\mathbf{V}_c = iq_c\mathbf{V}_c + \mathbf{U}_c.$$

Note that the applicability of this general theory requires a mirror symmetry $y \to -y$.

3.3. *Perturbed Ginzburg–Landau equation*

We limited ourselves first to localized imperfection around $y = 0$, which means that $G_l(y)$ decays for large y, and second to distributed imperfections that are nearly periodic with the critical wavenumber

$$\mathbf{G}_0(y) = \frac{1}{2}\sum_{n=0}^{\infty}(\mathbf{g}_n(y)\,e^{inq_c y} + \text{c.c.}) \tag{14}$$

where c.c. denotes the complex conjugate, the functions $\mathbf{g}_n(y)$ being slowly variable. Within this framework, we established (Damil and Potier-Ferry, 1991) that the bifurcation equation is the perturbed Ginzburg–Landau equation:

$$\mathbf{u}(y) = a(y)\mathbf{U}_c\,e^{iq_c y} + \text{c.c.} + \cdots \tag{15}$$

$$\frac{d^2a}{dy^2} + (P - P_c)\alpha_1 a + \alpha_2 a|a|^2 + \beta_1(y)a_0 = 0. \tag{16}$$

Next the localized imperfection induces a jump in the complex amplitude:

$$\left[\frac{da}{dy}(0)\right] = \frac{da}{dy}(0^+) - \frac{da}{dy}(0^-) = \gamma_1 a_1. \tag{17}$$

All the real coefficients α_1, α_2, γ_1 and the function $\beta_1(y)$ are given by general explicit formulae:

$$\alpha_1 = 2\Big/\frac{d^2P}{dq^2}(q_c) \tag{18}$$

$$\alpha_2 = -\alpha_1 b = \alpha_1\frac{\alpha_{30}}{\alpha_{11}} \tag{19}$$

$$\beta_1(y) = -\frac{1}{2}\frac{\langle \mathbf{g}_1(y), \mathbf{U}_c^*\rangle}{\langle \mathbf{V}_c, \mathbf{U}_c^*\rangle} \tag{20}$$

$$\gamma_1 = \frac{\langle \tilde{\mathbf{G}}_1(-q_c), \mathbf{U}_c^*\rangle}{\langle \mathbf{V}_c, \mathbf{U}_c^*\rangle} \tag{21}$$

$$\mathbf{V}_c = -i\frac{d\mathbf{U}q}{dq}(q_c) \tag{22}$$

where $\langle\cdot,\cdot\rangle$ is a hermitian product and $\mathbf{U}_c^*$ is the kernel of the adjoint operator $L^*(P_c) + iq_c$. From these formulae, it is clear that the coefficient α_1 is only deduced from the neutral stability curve $P(q)$ that follows from the eigenvalue problem:

$$L(P)\mathbf{U}_q = iq\mathbf{U}_q. \tag{23}$$

The function $\beta_1(y)$ is related to the linear stability problem (23) and to the distributed

imperfection. The coefficient γ_1 is related to the linear stability problem (23) and to the Fourier transform of the localized imperfection

$$\tilde{\mathbf{G}}_1(\omega) = \int_{-\infty}^{+\infty} \mathbf{G}_1(y)\, e^{i\omega y}\, dy \tag{24}$$

and α_2 is related to the standard imperfection sensitivity factor b.

4. INTERACTION OF DISTRIBUTED AND LOCALIZED IMPERFECTIONS

In this section we calculate the reduction of the critical load in the presence of both localized and distributed imperfections by solving the amplitude equation analytically.

In the case of a subcritical bifurcation, an imperfection transforms the bifurcation point $(P_c, 0)$ into a limit point (P_m, a_m), P_m being lower than P_c. The maximal load P_m will be deduced from the amplitude equation (16) together with the jump relation (17) at $y = 0$. Let us assume that β_1 is constant (as for instance with a modal imperfection). We seek only symmetric solutions with respect to the y-axis so that $a(y)$ is real. Hence $a(y)$ satisfies the following equations:

$$\frac{d^2a}{dy^2} + \alpha_1(P - P_c)a + \alpha_2 a^3 + a_0\beta_1 = 0 \tag{25}$$

$$\frac{da(0)}{dy} = \frac{\gamma_1}{2} a_1. \tag{26}$$

Hence eqns (25) and (26) govern the evolution of the amplitude $a(y)$. We seek solutions such that the amplitude is constant at infinity, i.e. out of the region where the localized imperfection is significant

$$a'(\infty) = 0, \quad a(\infty) = R. \tag{27}$$

Multiplying eqn (25) by a' and integrating gives

$$a'^2 + f(a) = C \tag{28}$$

$$f(a) = (P - P_c)\alpha_1 a^2 + \tfrac{1}{2}\alpha_2 a^4 + 2a_0\beta_1 a \tag{29}$$

where C is a constant of integration. The phase portrait of eqn (28) is shown in Fig. 2. Only the curves which go through the critical points F_1, S and F_2 are compatible with the assumption (27) of a constant amplitude in the large. The coordinates of the saddle point S and of the foci F_1 and F_2 are given by

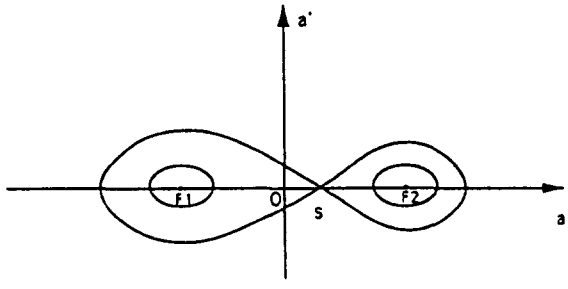

Fig. 2. Phase portrait of eqn (28).

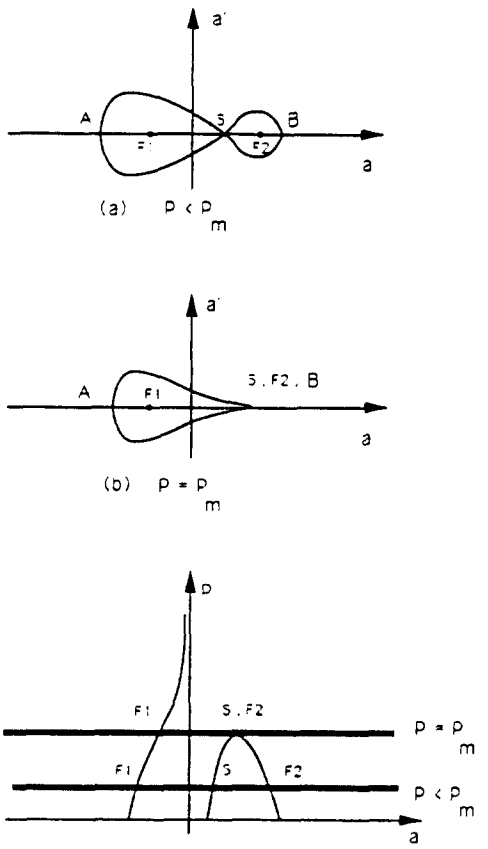

Fig. 3. The maximal load is reached when a loop disappears (case without localized imperfection).

$$f'(a) = 2[(P-P_c)\alpha_1 a + \alpha_2 a^3 + \beta_1 a_0] = 0. \tag{30}$$

Let us begin with the case without localized imperfections. The solutions of eqn (25) having constant amplitude correspond to the critical points F_1, S and F_2. There are also solutions corresponding to the paths AS and BS of Fig. 3. It is likely that only the solution corresponding to the saddle point is stable. If one increases the parameter P, the saddle point and one of the foci coincide, which corresponds to a maximal point on the load–amplitude curve (Fig. 3).

The presence of localized imperfections does not alter the saddle–saddle loop of the phase portrait, but the interesting solutions of eqns (25) and (26) are found by intersection of this loop with a straight line $a' = a'(0)$. So we find four solutions AS, BS, CS and DS, but only BS (respectively CS) seems to be stable in the case of Fig. 4a (respectively Fig. 4b). When we increase the load P, the curves which go through S deform and the points A, B, C and D move along the straight line $a' = a'$ (0), so the maximal load is reached at

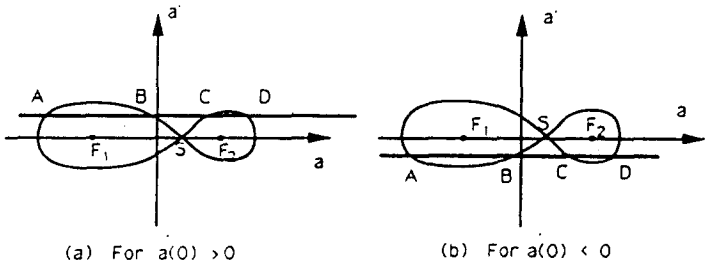

Fig. 4. Graphical discussion of eqns (25) and (26).

the coincidence of A and B. At this level the left orbit is a tangent to the straight line ($ABCD$) (see Fig. 5). The tangency condition gives

$$\frac{da'}{da} = 0. \tag{31}$$

Using eqn (27), eqn (28) reads

$$a'^2 + f(a) - f(R) = 0. \tag{32}$$

This equation can be written as:

$$a'^2 + (a-R)^2\left(\tfrac{1}{2}\alpha_2 R^2 + \alpha_2 aR + \tfrac{1}{2}\alpha_2 a^2 + \alpha_1(P-P_c)\right) = 0. \tag{33}$$

As was explained, in the presence of localized imperfection, the maximal point (P_m, a_m) is reached when the condition (31) holds, which leads to

$$\frac{\partial f}{\partial a}(a_m, P_m, a_0) = 0 \quad \text{and} \quad a'_m = a'(0). \tag{34a,b}$$

Thus a_m corresponds to one of the two foci F_1 or F_2 [see eqn (30)] and eqn (34a) gives

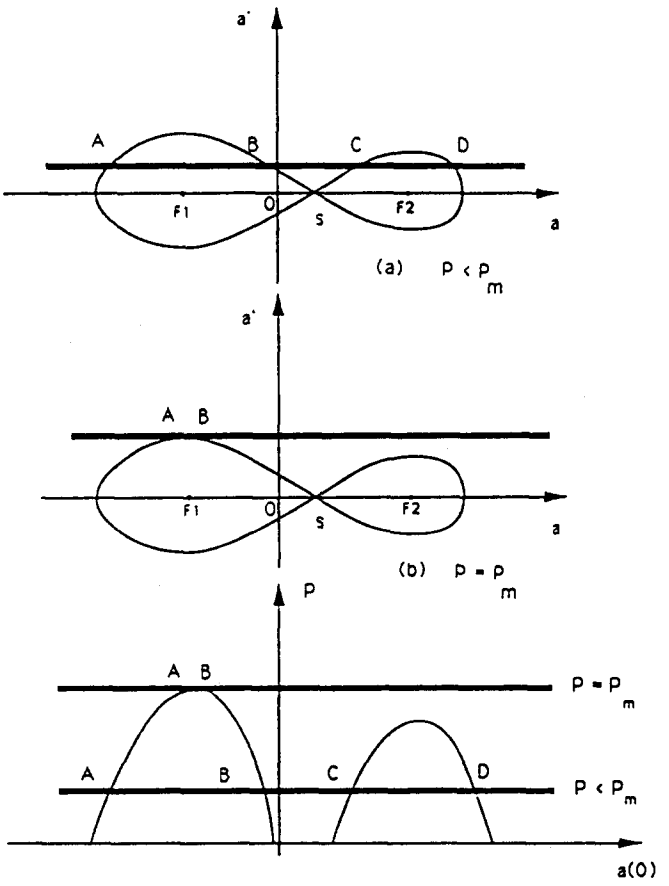

Fig. 5. The maximal load is reached when an orbit is at a tangent to the straight line (case with localized imperfection).

$$(P_m - P_c)\alpha_1 a_m + \alpha_2 a_m^3 + \beta_1 a_0 = 0. \tag{35}$$

Because of the relation,

$$(P_m - P_c)\alpha_1 R + \alpha_2 R^3 + \beta_1 a_0 = 0, \tag{36}$$

we get the maximal load P_m as a function of the maximal amplitude a_m and of the coordinate R of the saddle point S:

$$\begin{cases} P_m - P_c = \dfrac{\alpha_2}{\alpha_1}(a_m^2 + a_m R + R^2) \\ P_m - P_c = \dfrac{\alpha_2}{\alpha_1} a_m^2 + \beta_1 \dfrac{a_0}{\alpha_1}\dfrac{1}{a_m} = \dfrac{\alpha_2}{\alpha_1} R^2 + \dfrac{\beta_1 a_0}{\alpha_1}\dfrac{1}{R} \end{cases} \tag{37}$$

where a_m and R are solutions of the two equations [using eqns (33) and (34b)]:

$$\begin{cases} (a_m - R)^3(a_m + R) = \dfrac{2}{\alpha_2}(a'(0))^2 \\ a_m R(a_m + R) = \dfrac{\beta_1}{\alpha_2} a_0. \end{cases} \tag{38}$$

Finally, the maximal load P_m can be deduced by solving eqn (38) according to the sign of $a'(0)$.

4.1. *First case*: a'(0) < 0 (Fig. 6)

In this case, the localized imperfection is roughly in-phase with the distributed one, and we have $a_m > R > 0$. Let

$$a_m = kR. \tag{39}$$

Remark that if $k = 1$, then $a_m = R$ and we have the case without localized imperfection [see eqn (38) and Fig. 3]. If $k \gg 1$, only the localized imperfection is significant.

Substituting for a_m from eqn (39) into eqn (38) yields

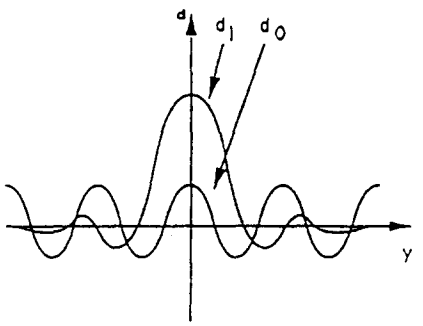

Fig. 6. The localized and the distributed imperfections are in-phase.

$$\begin{cases} R^4(k-1)^3(k+1) = \dfrac{2}{\alpha_2}(a'(0))^2 \\ R^3 k(k+1) = \dfrac{\beta_1}{\alpha_2} a_0. \end{cases} \tag{40a,b}$$

From this last equation, one gets, after dropping R

$$h(k) = \frac{(k-1)^3}{k^{4/3}(k+1)^{1/3}} = 2\frac{\alpha_2^{1/3}}{(\beta_1 a_0)^{4/3}}(a'(0))^2. \tag{41}$$

In Fig. 7, we have plotted the graph of the function h. One sees that eqn (41) always admits a solution $k > 1$. Thus, for any $a'(0) < 0$, we can calculate the reduction of critical load in a nearly closed form [using eqns (41), (40), (37) and (26)]:

$$k = h^{-1}\left(2\frac{\alpha_2^{1/3}}{(\beta_1 a_0)^{4/3}}\left(\frac{\gamma_1}{2}a_1\right)^2\right)$$

$$a_m = kR \quad \text{and} \quad R = \left(\frac{\beta_1}{\alpha_2}a_0\frac{1}{k(k+1)}\right)^{1/3}$$

$$P_c - P_m = \frac{\alpha_2^{1/3}}{\alpha_1}(\beta_1 a_0)^{2/3}\frac{1+k+k^2}{[k(k+1)]^{2/3}}. \tag{42}$$

Let us examine two important cases. If there is no localized imperfection, $a_1 = 0$ and then $a'(0) = 0$. From eqn (40a), one gets $k = 1$ and from eqn (42) we get the same formula as in Koiter's theory:

$$P_c - P_m = \frac{3}{2^{2/3}}\frac{\alpha_2^{1/3}}{\alpha_1}(\beta_1 a_0)^{2/3}. \tag{43}$$

If only the localized imperfection is significant (i.e. k is large), eqns (41) and (42) lead to the formula given in Amazigo *et al.* (1970) for a beam buckling problem:

$$P_c - P_m = \frac{\sqrt{2\alpha_2}}{\alpha_1}\frac{|\gamma_1|}{2}a_1. \tag{44}$$

Both localized and distributed imperfections must be taken into account in the range where the imperfection ratio $a_1/a_0^{2/3}$ is of the order of unity. Notice that this implies a localized part of the imperfection much larger than the distributed part. In this case we propose the formulae (42) that can be inverted numerically.

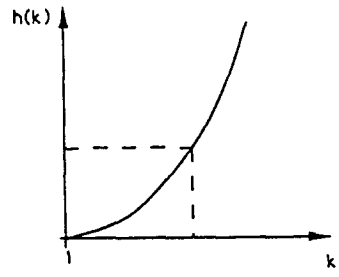

Fig. 7. Graph of the function h.

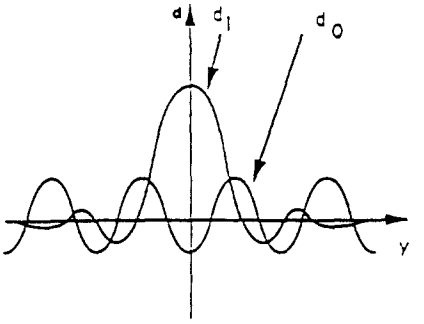

Fig. 8. The localized and distributed imperfections are out-of-phase.

4.2. *Second case*: a'(0) > 0 (Fig. 8)

Here we consider the case of an out-of-phase localized imperfection (Fig. 8). In this case the maximal load can be reached by two different manners in the phase portrait. First, the line $a' = a'(0)$ becomes a tangent to the saddle–saddle loop, as in the previous case. This occurs when the instability is governed mainly by the localized imperfection. Second, the saddle–saddle loop can shrink by coalescence of the saddle and of one focus. In this case, the instability does not start in the region of the localized imperfection, which has no influence on the maximal load, and the classical reduction formula (43) is applicable.

Let us compute the maximal load when the localized imperfection has an influence. Let ($a_m < 0, R > 0$)

$$a_m = -kR, \quad k > 0. \tag{45}$$

Substituting for a_m from eqn (45) into the tangency condition (38) yields

$$\begin{cases} R^4(k+1)^3(k-1) = \dfrac{2}{\alpha_2}(a'(0))^2 \\ R^3k(k-1) = \dfrac{\beta_1}{\alpha_2}a_0. \end{cases} \tag{46a,b}$$

From eqn (46a), it is seen that $k > 1$. After dropping R, eqns (46) lead to

$$h_2(k) = \frac{(k+1)^3}{k^{4/3}(k-1)^{1/3}} = 2\frac{\alpha_2^{1/3}}{(\beta_1 a_0)^{4/3}}(a'(0))^2. \tag{47}$$

In Fig. 9, we display the graph of the function h_2. For given $h_2(k)$, eqn (47) does not always admit a solution, due to the existence of a minimum of $h_2(k)$. The localized imperfection amplitude must meet the condition

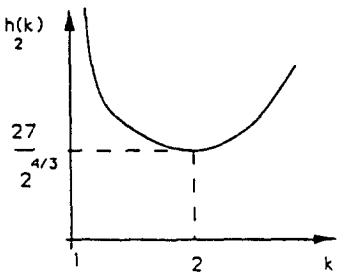

Fig. 9. Graph of the function h_2.

$$2\frac{\alpha_2^{1/3}}{(\beta_1 a_0)^{4/3}}\left(\frac{\gamma_1}{2}a_1\right)^2 > \frac{27}{2^{4/3}} \approx 10. \tag{48}$$

If the condition (48) does not hold, the instability is not due to the localized imperfection and the reduction formula (43) yields the maximal load.

If the condition (48) holds, two values of k seem to be admissible (Fig. 9). Nevertheless, the solutions $k < 2$ give maximal loads that are greater than the classical maximal load from eqn (43) and therefore they do not correspond to admissible values. So the reduction formulae are

$$k = h_2^{-1}\left(2\frac{\alpha_2^{1/3}}{(\beta_1 a_0)^{4/3}}\left(\frac{\gamma_1}{2}a_1\right)^2\right) \quad \text{and} \quad k > 2$$

$$R^3 = \frac{\beta_1 a_0}{\alpha_2 k(k-1)}$$

$$P_c - P_m = \frac{\alpha_2}{\alpha_1}R^2 + \frac{\beta_1 a_0}{\alpha_1}\frac{1}{R}. \tag{49}$$

5. APPLICATION TO BUCKLING OF CYLINDRICAL SHELLS UNDER EXTERNAL PRESSURE

5.1. *Calculation of the envelope equation*

In this section we apply the latter formulae to calculate the reduction of the critical pressure of a cylinder with a large Batdorf parameter Z and a not too large aspect ratio L/R, in the presence of an initial imperfection localized close to $y = 0$ (Fig. 10) and/or a modal imperfection. We begin by the computation of the coefficients of the envelope equation (16) as well as the jump conditions (17).

We shall consider two shapes for the localized imperfections:

Localized imperfection: shape 1 (Fig. 11)

$$d_1(x, y) = d(x)d_1(y) = d(x)\exp[-(y/c)^2], \quad c > 0. \tag{50}$$

Localized imperfection: shape 2 (Fig. 12)

$$d_1(x, y) = d(x)d_1(y) = d(x)\cos q_c y \exp[-(y/c)^2], \quad c > 0. \tag{51}$$

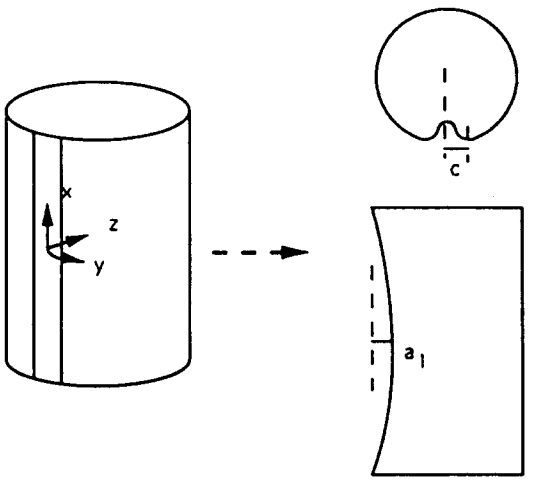

Fig. 10. Shape of the localized imperfection.

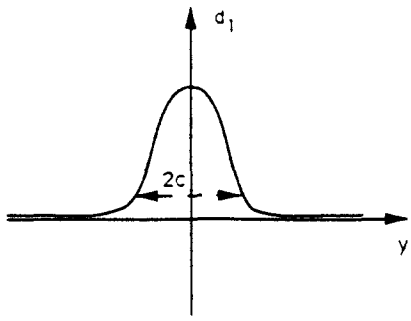

Fig. 11. Localized imperfection (shape 1).

The modal imperfection has the following shape:

$$d_0(x, y) = d(x) \cos q_c y. \tag{52}$$

The real number c characterizes the width of the region where the localized imperfection is not too small. In what follows, it will be compared to the circumferential wavelength of the buckling mode. For these examples the localized and distributed imperfections will be in-phase. The reduction of the critical pressure is then given by formulae (42), (43) or (44). To apply these formulae we have to compute α_1, α_2, β_1 and γ_1, which are given by eqns (18)–(21) and the solution of the neutral stability problem (23). Here the linear operator is given by:

$$L(P) = \begin{bmatrix} 0 & 0 & 0 & 0 & 1 & 0 & 0 & 0 \\ 0 & 0 & 0 & 0 & 0 & 1 & 0 & 0 \\ 0 & 0 & 0 & 0 & 0 & 0 & 1 & 0 \\ 0 & 0 & 0 & 0 & 0 & 0 & 0 & 1 \\ 0 & 0 & 1 & 0 & 0 & 0 & 0 & 0 \\ 0 & 0 & 0 & 1 & 0 & 0 & 0 & 0 \\ 0 & \frac{1}{DR}\partial_x^2 & -\frac{PR}{D} & 0 & 0 & 0 & 0 & 0 \\ -\frac{Eh}{R}\partial_x^2 & 0 & 0 & 0 & 0 & 0 & 0 & 0 \end{bmatrix}. \tag{53}$$

Then the well-known stability problem (23) is solved by the following eigenvector and adjoint eigenvector:

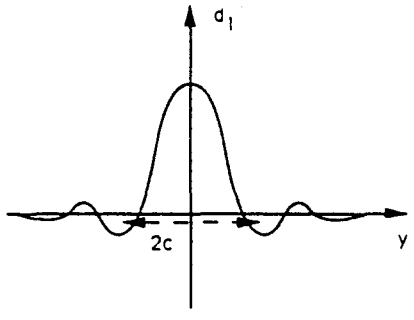

Fig. 12. Localized imperfection (shape 2).

$$\begin{cases} {}^{t}\mathbf{U}_q = \{p_1, p_2, -q^2 p_1, -q^2 p_2, iqp_1, iqp_2, -iq^3 p_1, -iq^3 p_2\} \\ P(q) = \dfrac{D}{R}\left(q^2 + \eta \dfrac{r^4}{q^6}\right) \end{cases} \tag{54a,b}$$

$${}^{t}\mathbf{U}_q^* = \left\{p_2, p_1, \frac{q^6}{\eta r^4} p_2, -\frac{1}{q^2} p_1, \frac{i}{q} p_2, \frac{i}{q} p_1, \frac{iq^5}{\eta r^4} p_2, -\frac{i}{q^3} p_1\right\} \tag{55}$$

where

$$\eta = 12 Z^2 \frac{\pi^4}{L^8}, \quad Z = \frac{L^2}{Rh}\sqrt{1-\nu^2}. \tag{56}$$

The number r in eqns (54) and (55) depends on the boundary conditions [see (61)]. The functions $p_1(x)$ and $p_2(x)$ are solutions of the linear differential equations

$$\begin{cases} \left(q^4 - \dfrac{PR}{D} q^2\right) p_1(x) - \dfrac{1}{DR} \partial_x^2 p_2(x) = 0 \\ q^4 p_2(x) + \dfrac{Eh}{R} \partial_x^2 p_1(x) = 0. \end{cases} \tag{57}$$

The boundary conditions of eqn (57) are deduced from eqns (5) or (6):

1. If there is no axial restraint ($N_x = 0$)

$$p_1\left(\pm \frac{L}{2}\right) = \partial_x^2 p_1\left(\pm \frac{L}{2}\right) = 0. \tag{58}$$

2. If there is an axial restraint ($u = 0$)

$$p_1\left(\pm \frac{L}{2}\right) = \partial_x p_1\left(\pm \frac{L}{2}\right) = 0. \tag{59}$$

One finds the critical functions [the critical buckling mode being $w(x, y) = 2p_1(x) \cos q_c y$]

$$\begin{cases} p_1(x) = \alpha \cos \dfrac{r\pi x}{L} + \beta \cosh \dfrac{r\pi x}{L} \\ p_2(x) = -\dfrac{Eh}{R} \dfrac{1}{q_c^4} \partial_x^2 p_1(x) \end{cases} \tag{60a,b}$$

with

$$\begin{cases} r = 1.505619 \\ \beta = \dfrac{1}{2} \dfrac{\sin(r\pi/2)}{\sin(r\pi/2) + \sinh(r\pi/2)}, \quad \alpha = \dfrac{1}{2} \dfrac{\sinh(r\pi/2)}{\sin(r\pi/2) + \sinh(r\pi/2)} \end{cases} \quad \text{or} \quad \begin{cases} r = 1 \\ \alpha = \frac{1}{2}, \quad \beta = 0 \end{cases} \tag{61}$$

according to whether there is an axial restraint ($u = 0$) or not ($N_x = 0$). From the neutral stability curve (54b) we get the following critical values:

$$q_c^8 = 3\eta r^4$$

$$P_c = P(q_c) = \frac{4}{3}\frac{D}{R}q_c^2$$

$$\frac{d^2P}{dq^2}(q_c) = 16\frac{D}{R}. \tag{62a-c}$$

Equations (54a) and (55) yield the following vectors:

$$^tU_c = \{p_1, p_2, -q_c^2 p_1, -q_c^2 p_2, iq_c p_1, iq_c p_2, -iq_c^3 p_1, -iq_c^3 p_2\}$$

$$^tU_c^* = \left\{p_2, p_1, \frac{3}{q_c^2}p_2, \frac{-1}{q_c^2}p_1, \frac{i}{q_c}p_2, \frac{i}{q_c}p_1, \frac{3i}{q_c^3}p_2, -\frac{i}{q_c^3}p_1\right\}$$

$$^tV_c = -i\frac{d}{dq}{}^tU_q(q_c) = \left\{0, \frac{4i}{q_c}p_2, 2iq_c p_1, -2iq_c p_2, p_1, 3p_2, 3q_c^2 p_1, -q_c^2 p_2\right\} \tag{63}$$

which permits us to get the following hermitian product:

$$\langle V_c, U_c^* \rangle = \frac{24}{q_c} i \int_{-L/2}^{L/2} p_1(x)p_2(x)\,dx. \tag{64}$$

The vector G_0, related to the distributed imperfection, is

$$^tG_0(x, y) = \left\{0, 0, 0, 0, 0, 0, \frac{P_c R}{D}q_c^2 d_0(x, y), 0\right\}.$$

As the distributed imperfection is modal [$d(x) = 2p_1(x)$ in (52)], we get

$$^tg_1 = \left\{0, 0, 0, 0, 0, 0, \frac{P_c R}{D}q_c^2 p_1(x), 0\right\}.$$

By using eqns (63) and (64), formula (20) leads to the coefficient β_1 related to the modal imperfection:

$$\beta_1 = \frac{P_c R}{8D} = \tfrac{1}{6}q_c^2. \tag{65}$$

The vector G_1, related to the localized imperfections, is

$$^tG_1(x, y) = \left\{0, 0, 0, 0, 0, 0, -\frac{P_c R}{D}\partial_y^2 d_1(x, y), 0\right\}.$$

By means of the Fourier transform defined in eqn (24), we get the Fourier transform of G_1 with respect to y:

$$^t\tilde{G}_1(x, \omega) = \left\{0, 0, 0, 0, 0, 0, \frac{P_c R}{D}\omega^2 d(x)\tilde{d}_1(\omega), 0\right\}.$$

Thus

$$\langle \tilde{\mathbf{G}}_1(-q_c), \mathbf{U}_c^* \rangle = -3i \frac{P_c R}{q_c D} \bar{d}_1(-q_c) \int_{-L/2}^{L/2} d(x) p_2(x)\, dx. \tag{66}$$

In order to simplify the computations we limit ourselves to $d(x) = 2p_1(x)$. With this choice, formula (21) gives the coefficient γ_1 [using eqns (62b), (64) and (66)]:

$$\gamma_1 = -\tfrac{1}{3} q_c^2 \bar{d}_1(-q_c). \tag{67}$$

From eqn (62c), formula (18) gives the coefficient α_1:

$$\alpha_1 = \frac{1}{8} \frac{R}{D}. \tag{68}$$

The last coefficient $\alpha_2 = -\alpha_1 b$ will be deduced from a classical bifurcation analysis. The factor b has been computed in the Appendix for the two classes of boundary conditions $u = 0$ and $N_x = 0$. We obtain

$$b = -3.4644 \frac{Eh}{q_c^2 R} \left(\frac{\pi}{L}\right)^4 \quad \text{or} \quad b = -1.0732 \frac{Eh}{q_c^2 R} \left(\frac{\pi}{L}\right)^4 \tag{69}$$

$$\alpha_2 = 0.43305 \frac{Eh}{D} \frac{1}{q_c^2} \left(\frac{\pi}{L}\right)^4 \quad \text{or} \quad \alpha_2 = 0.13415 \frac{Eh}{D} \frac{1}{q_c^2} \left(\frac{\pi}{L}\right)^4 \tag{70}$$

depending on whether there is an axial restraint ($u = 0$) or not ($N_x = 0$).

For these two cases, the numerical coefficients of the envelope equation (16) are given by eqns (65), (68) and (70), while the coefficient γ_1 of the jump condition (17) is given by eqn (67). Next, the reduction of critical pressure will be deduced from the analytical solution of Section 4.

5.2. *Reduction formulae for the critical pressure*

We propose analytical formulae for the reduction of the critical buckling pressure of cylindrical shells ($Z \geqslant 500$ and a not too large L/R) due to various types of imperfections.

5.2.1. *Only modal imperfection.* The classical formula (43) leads to the following reduction:

$$P_c - P_m = \frac{3}{2^{2/3}} \left(\frac{\alpha_2}{\alpha_1}\right)^{1/3} \left(\frac{\beta_1}{\alpha_1} a_0\right)^{2/3} = \frac{3}{2^{2/3}} (-b)^{1/3} (P_c a_0)^{2/3}, \tag{71}$$

which can be written as:

$$\begin{cases} \dfrac{P_m}{P_c} = 1 - 4.7511 \dfrac{(1-\nu^2)^{1/3}}{Z^{1/3}} \left(\dfrac{a_0}{h}\right)^{2/3} & \text{if} \quad N_x = 0 \\ \dfrac{P_m}{P_c} = 1 - 5.3452 \dfrac{(1-\nu^2)^{1/3}}{Z^{1/3}} \left(\dfrac{a_0}{h}\right)^{2/3} & \text{if} \quad u = 0. \end{cases} \tag{72}$$

These analytical formulae have been obtained using the approximate Donnell equations (7). Comparison between the formulae (72), which were deduced from the inextensional approximation, and the exact formulae, which were obtained numerically from eqns (1)

Table 1. $R/h = 100$, $a_0/h = 0.2$; the reduction of critical pressure as a function of Z and boundary conditions: comparison of approximate formula with exact formula

	Z			
	215		858	
B.C.	Approximate	Exact	Approximate	Exact
C3	0.737	0.748	0.834	0.834
S3		0.757		0.836
C4		0.747		0.834
S4		0.766		0.840
C1	0.704	0.746	0.814	0.830
S1		0.754		0.832
C2		0.749		0.832
S2		0.752		0.837

and (71), are given in Table 1 for $a_0/h = 0.2$, $R/h = 100$, and for various boundary conditions.

For large Z formulae (72) are sufficiently accurate in the case $N_x = 0$ and they induce at most an error of 3% in the case $u = 0$. A similar error is obtained for a smaller Z in the case $N_x = 0$. Furthermore, the convergence is good when Z increases.

5.2.2. *Only localized imperfection.* If there is only localized imperfection, the reduction of critical pressure is given by eqn (44), which leads to:

$$\begin{cases} \dfrac{P_m}{P_c} = 1 - 2.3013 \dfrac{\sqrt{1-\nu^2}}{\sqrt{Z}} q_c \bar{d}_1(-q_c) \dfrac{a_1}{h}, & \text{if} \quad N_x = 0 \\ \dfrac{P_m}{P_c} = 1 - 2.7462 \dfrac{\sqrt{1-\nu^2}}{\sqrt{Z}} q_c \bar{d}_1(-q_c) \dfrac{a_1}{h}, & \text{if} \quad u = 0. \end{cases} \tag{73}$$

Let us examine the two shapes given by eqns (50) and (51) for the localized imperfection. For the first shape, by using the following Fourier transform

$$\bar{d}_1(\omega) = c\sqrt{\pi} \exp\left(-\left(\frac{c}{2} q_c \omega\right)^2\right), \quad q_c = (6Z)^{1/4} \sqrt{r\pi} \frac{1}{L},$$

we get

$$\begin{cases} \dfrac{P_m}{P_c} = 1 - d_{1N} \dfrac{a_1}{h} & \text{if} \quad N_x = 0 \\ \dfrac{P_m}{P_c} = 1 - d_{1u} \dfrac{a_1}{h} & \text{if} \quad u = 0 \end{cases} \tag{74}$$

$$\begin{cases} d_{1N} = 11.3152 \dfrac{(1-\nu^2)^{1/2}}{Z^{1/4}} \dfrac{c}{L} \exp\left(-1.9238 \sqrt{Z} \left(\dfrac{c}{L}\right)^2\right) \\ d_{1u} = 16.5683 \dfrac{(1-\nu^2)^{1/2}}{Z^{1/4}} \dfrac{c}{L} \exp\left(-2.8965 \sqrt{Z} \left(\dfrac{c}{L}\right)^2\right). \end{cases} \tag{75}$$

For the second shape, the Fourier transform is

$$\bar{d}_1(\omega) = c\frac{\sqrt{\pi}}{2}\left[\exp\left(-\left(\frac{c}{2}q_c(\omega+1)\right)^2\right)+\exp\left(-\left(\frac{c}{2}q_c(\omega-1)\right)^2\right)\right].$$

This leads to the following formulae:

$$\begin{cases} \dfrac{P_m}{P_c} = 1-d_{2N}\dfrac{a_1}{h} & \text{if} \quad N_x = 0 \\ \dfrac{P_m}{P_c} = 1-d_{2u}\dfrac{a_1}{h} & \text{if} \quad u = 0 \end{cases} \tag{76}$$

$$\begin{cases} d_{2N} = 5.6576\dfrac{(1-\nu^2)^{1/2}}{Z^{1/4}}\dfrac{c}{L}\left[1+\exp\left(-7.6952\sqrt{Z}\left(\dfrac{c}{L}\right)^2\right)\right] \\ d_{2u} = 8.28415\dfrac{(1-\nu^2)^{1/2}}{Z^{1/4}}\dfrac{c}{L}\left[1+\exp\left(-11.586\sqrt{Z}\left(\dfrac{c}{L}\right)^2\right)\right]. \end{cases} \tag{77}$$

In Fig. 13, we give the evolution of the slope of the straight lines defined by eqns (75) and (76) as a function of c/L for various values of the geometrical parameter Z and for the two classes of boundary conditions. It is seen that for large c/L, the second shape defined by eqn (51) generally reduces the critical pressure more than the first shape defined by eqn (50). As for the modal imperfection, the reduction is generally larger in the case of an axial restraint ($u = 0$) than for no axial restraint ($N_x = 0$).

5.2.3. *Interaction of localized and modal imperfections.* If both localized and distributed imperfections are significant, the reduction of critical pressure is given by formulae (42). For the purpose of comparison, we choose the second type of localized imperfection defined by eqn (51). With this choice formulae (42) lead to the following reduction:

$$\frac{P_m}{P_c} = 1-\delta_3\frac{(1-\nu^2)^{1/3}}{Z^{1/3}}\left(\frac{a_0}{h}\right)^{2/3}\frac{1+k+k^2}{[k(k+1)]^{2/3}} \tag{78}$$

where k satisfies the algebraic equation ($k > 1$)

$$\frac{(k-1)^3}{k^{4/3}(k+1)^{1/3}} = \delta_1(1-\nu^2)^{1/3}Z^{1/6}\left(\frac{c}{L}\right)^2\left[1+\exp\left(-\delta_2\sqrt{Z}\left(\frac{c}{L}\right)^2\right)\right]\frac{(a_1/h)^2}{(a_0/h)^{4/3}} \tag{79}$$

$$\begin{bmatrix}\delta_1 = 8.579 \\ \delta_2 = 11.586 \\ \delta_3 = 2.828\end{bmatrix} \quad \text{or} \quad \begin{bmatrix}\delta_1 = 5.065 \\ \delta_2 = 7.695 \\ \delta_3 = 2.514\end{bmatrix} \tag{80}$$

depending on whether there is an axial restraint ($u = 0$) or not ($N_x = 0$). The interaction between localized and modal imperfections depends on c/L and on the boundary conditions, as shown in Fig. 14.

Figure 14a shows how the interaction between both types of imperfections significantly reduces the buckling pressure. The case that is presented corresponds to a localized imperfection that is concentrated on half a buckle. Here we get the same reduction of 19% with a much greater localized imperfection than with a modal imperfection ($a_1/h = 2$ and $a_0/h = 0.2$). With both imperfections, the same reduction is obtained for $a_0/h = 0.12$ and $a_1/h = 1$. If the localized imperfection is significant on one or two buckles, the reduction is more severe (Fig. 14b). Furthermore, the structure is more imperfection sensitive with the boundary condition $u = 0$ than with $N_x = 0$ (Fig. 14c).

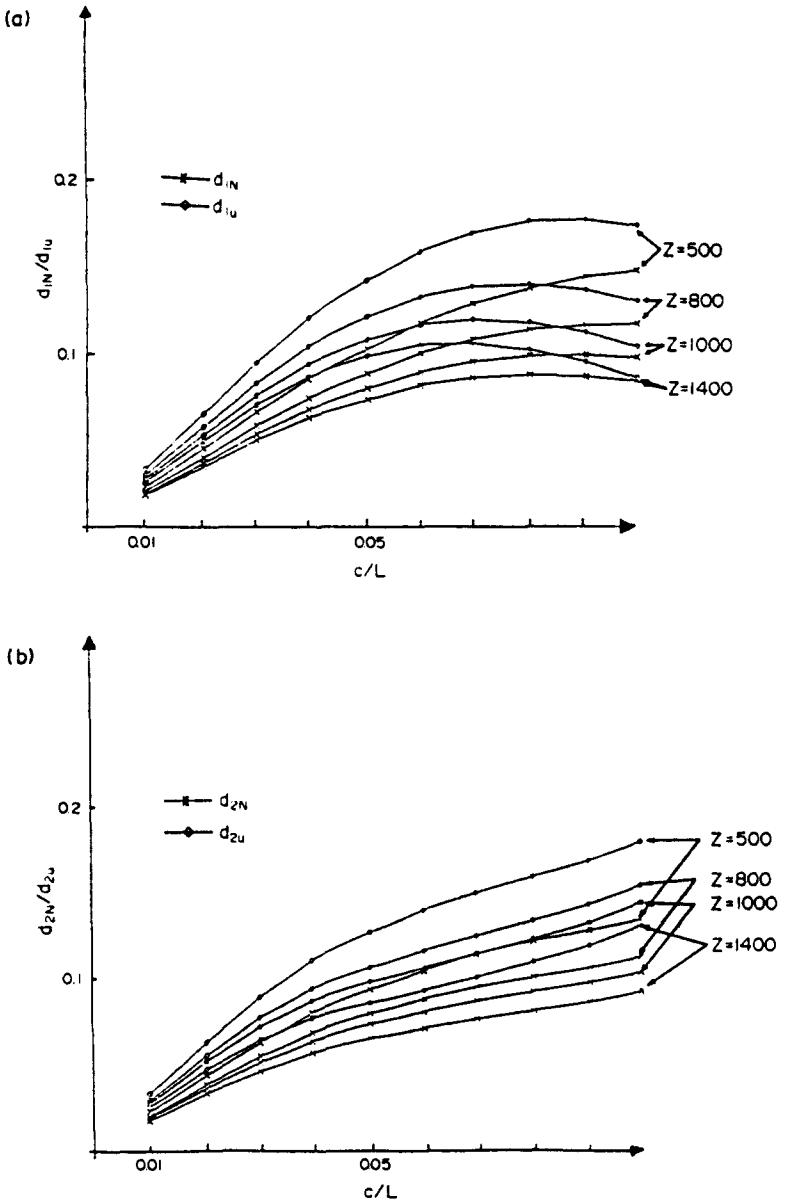

Fig. 13. Localized imperfection sensitivity coefficient as a function of the shape of the imperfection (c/L, shape 1 or shape 2), of the geometry of the shell (Z) and of the boundary conditions for $\nu = 0.3$. (a) For localized imperfection shape 1. (b) For localized imperfection shape 2.

6. CONCLUSION

We have discussed the imperfection sensitivity of elastic cylindrical shells under external pressure. We used a simplified analysis (Abdelmoula and Potier-Ferry, 1991) derived from Donnell equations, which limits the applications to a sufficiently large Batdorf parameter Z and a not too large ratio L/R. In this case, the wavenumber is not too small, which permits one to distinguish between distributed and localized imperfections. These two types of imperfections were taken into account.

Closed form formulae (72), (74) and (76) were established for the reduction of buckling pressure due to distributed or localized imperfections. The interaction between the two types of imperfection can be accounted for by formulae (78) and (79). The reduction of buckling pressure depends mainly on the Batdorf parameter, on the characteristics of the imperfections and on the axial boundary conditions.

The classical post-buckling theory cannot be applied in the presence of localized

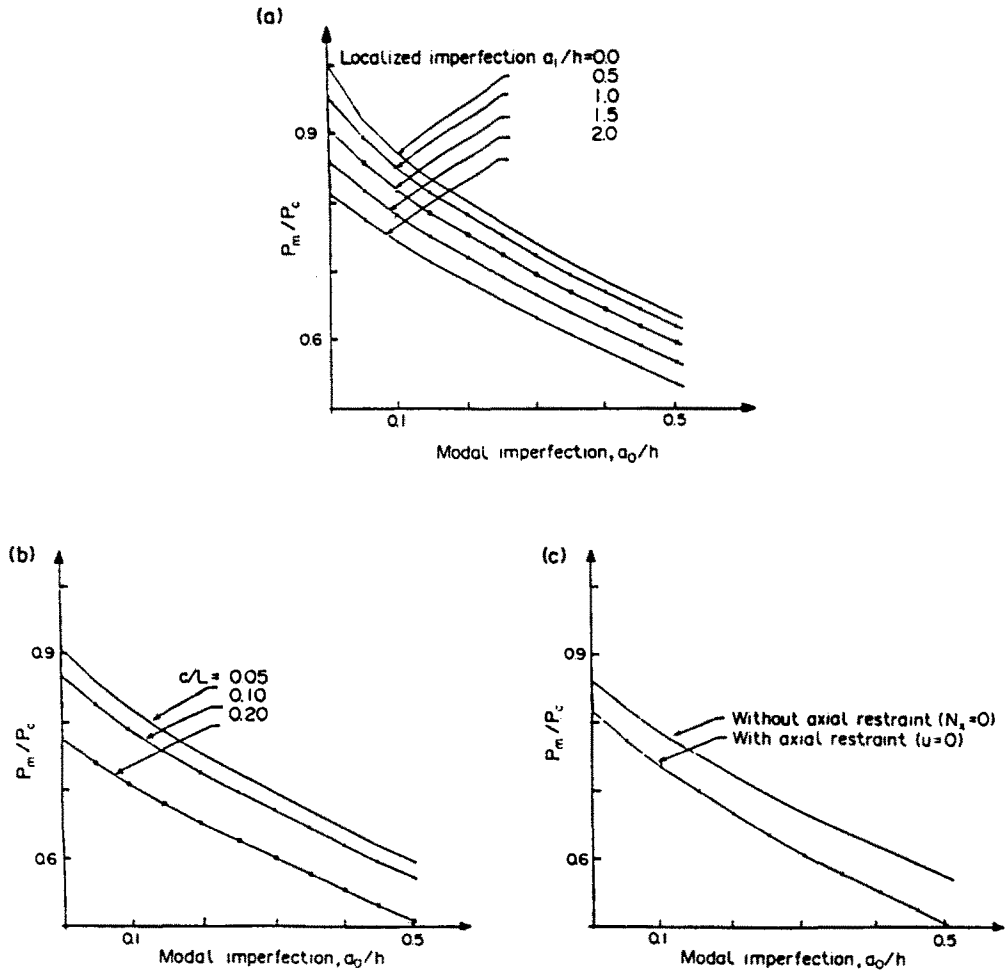

Fig. 14. Reduction of the critical pressure in the presence of a modal imperfection (amplitude a_0) and of a localized imperfection (amplitude a_1) for $Z = 500$ and $\nu = 0.3$. (a) For $c/L = 0.05$ and no axial restraint ($N_x = 0$). (b) For $a_1/h = 1.0$ and no axial restraint ($N_x = 0$). (c) For $a_1/h = 1.0$ and $c/L = 0.1$.

imperfection. A cellular bifurcation analysis is necessary in that respect. The general theory that we recently established for this purpose (Damil and Potier-Ferry, 1991) makes this type of study easier.

REFERENCES

Abdelmoula, R. and Potier-Ferry, M. (1991). Influence of boundary conditions on the buckling of cylindrical elastic shells: an asymptotic analysis. Preprint.

Amazigo, J. C. and Frazer, W. B. (1971). Buckling under external pressure of cylindrical shells with dimple shaped initial imperfections. *Int. J. Solids Structures* 7, 883–900.

Amazigo, J. C., Budiansky, B. and Carrier, G. F. (1970). Asymptotic analysis of the buckling of imperfect columns on nonlinear elastic foundations. *Int. J. Solids Structures* 6, 1341–1356.

Arbocz, J., Potier-Ferry, M., Singer, J. and Tvergaard, V. (1987). *Buckling and Post-buckling*, Lecture Notes in Physics. Springer, Berlin.

Budiansky, B. (1974). Theory of buckling and post-buckling behaviour of elastic structures. *Adv. Appl. Mech.* 14, 1–65.

Bushnell, D. (1985). *Computerized Buckling Analysis of Shells*. Martinus Nijhoff, The Netherlands.

Damil, N. and Potier-Ferry, M. (1991). Amplitude equations for cellular instabilities. *Dynamics and Stability of Systems* (in press).

Dubas, P. and Van De Pite, D. (1987). *ECCS Colloquium on Stability of Plate and Shell Structures*, Ghent University.

Hui, D., Birman, V. and Bushnell, D. (1989). Recent developments in buckling of structures. ASME PVP-83 and AD-18, Winter Annual Meeting, San Francisco.

Koiter, W. T. (1945). On the stability of elastic equilibrium. Thesis, Delft. English translation: NASA Techn. Transl. F10, 833 (1967).
Newell, A. C. and Whitehead, J. A. (1969). Finite band width, finite amplitude convection. *J. Fluid Mech.* **38**, 279–303.
Potier-Ferry, M. (1987). In *Buckling and Post-buckling* (Edited by J. Arbocz *et al.*), Lecture Notes in Physics, pp. 1–82. Springer, Berlin.
Segel, L. (1969). Distant sidewalls cause slow amplitude modulation of cellular convection. *J. Fluid Mech.* **38**, 203–224.
Thompson, J. M. T. and Hunt, G. W. (1973). *A General Theory for Elastic Stability*. John Wiley, New York.
Yamaki, N. (1984). *Elastic Stability of Circular Cylindrical Shells*. North-Holland, Amsterdam.

APPENDIX

In this Appendix we compute the classical b factor of the standard bifurcation theory. The b factor is given by (see for example Budiansky, 1974)

$$b = -\frac{\alpha_{30}}{\alpha_{11}} = -\frac{(\mathscr{L}_4(\mathbf{u}_1) - \mathscr{L}_2(\hat{\mathbf{v}}))}{2\dfrac{\mathrm{d}\mathscr{L}_2}{\mathrm{d}P}(\mathbf{u}_1)} \tag{A1}$$

where we have used the notation from Potier-Ferry (1987). The Reissner-type functional in eqn (8) can be rewritten as:

$$\mathscr{L}(P, \mathbf{u}) = \mathscr{L}_2(P, \mathbf{u}) + \mathscr{L}_3(P, \mathbf{u}). \tag{A2}$$

Here $\mathbf{u} = {}^t\{w, f\}$. The functional $\mathscr{L}_m(\mathbf{u})$ is homogeneous of degree m. We also use the functional $\mathscr{L}_{21}(\ldots)$ that is homogeneous of degree 2 (resp. 1) with respect to its first (resp. second) arguments and that is the derivative of $\mathscr{L}_1(.)$. Note that for the shell problem the functional $\mathscr{L}_4$ is zero and the buckling mode $\mathbf{u}_1$ is given by

$$\mathbf{u}_1 = \begin{pmatrix} w_1 \\ f_1 \end{pmatrix} = 2\begin{pmatrix} p_1(x)\cos q_c y \\ p_2(x)\cos q_c y \end{pmatrix}. \tag{A3}$$

The vector $\mathbf{v} = {}^t\{w, f\}$ is the solution of the variational problem (see Potier-Ferry, 1987):

$$-2\mathscr{L}_{11}(\hat{\mathbf{v}}, \delta\mathbf{v}) = \tfrac{1}{2}\mathscr{L}_{21}(\mathbf{u}_1, \delta\mathbf{v}) \quad \forall\, \delta\mathbf{v}. \tag{A4}$$

This leads to the following problem for $\hat{w}(x, y)$ and $\hat{f}(x, y)$:

$$\begin{cases} D\partial_y^4\hat{w} + P_c R\partial_y^2\hat{w} - \dfrac{1}{R}\partial_x^2\hat{f} = [w_1, f_1] \\ \dfrac{1}{Eh}\partial_y^4\hat{f} + \dfrac{1}{R}\partial_x^2\hat{w} = -\tfrac{1}{2}[w_1, w_1]. \end{cases} \tag{A5}$$

Using the buckling mode given by (A3), the problem (A5) can be rewritten as

$$\begin{cases} D\partial_y^4\hat{w} + P_c R\partial_y^2\hat{w} - \dfrac{1}{R}\partial_x^2\hat{f} = -2q_c^2[p_1''p_2 + p_1p_2'' - 2p_1'p_2']\cos 2q_c y - 2q_c^2(p_1p_2)'' \\ \dfrac{1}{Eh}\partial_y^4\hat{f} + \dfrac{1}{R}\partial_x^2\hat{w} = -2q_c^2[p_1p_1'' - (p_1')^2]\cos 2q_c y + q_c^2(p_1^2)'' \end{cases} \tag{A6}$$

where $(\;)'$ designates a differentiation with respect to x. The solution of (A6), which is orthogonal to the buckling mode $\mathbf{u}_1$, is in the form

$$\begin{aligned} \hat{w}(x, y) &= \hat{w}_0(x) + \hat{w}_2(x)\cos 2q_c y \\ \hat{f}(x, y) &= \hat{f}_0(x) + \hat{f}_2(x)\cos 2q_c y \end{aligned} \tag{A7}$$

where w_0, w_2, f_0, f_2 are solutions of:

$$\begin{cases} -\dfrac{1}{R}\hat{f}_0'' = -2q_c^2(p_1p_2)'' \\ \dfrac{1}{R}\hat{w}_0'' = q_c^2(p_1^2)'' \end{cases} \tag{A8}$$

and

$$\begin{cases} \dfrac{32}{3} q_c^4 D\hat{w}_2 - \dfrac{1}{R}\hat{f}_2'' = -2q_c^2(p_1''p_2 + p_1p_2'' - 2p_1'p_2') \\ \dfrac{16}{Eh} q_c^4 \hat{f}_2 + \dfrac{1}{R}\hat{w}_2'' = 2q_c^2(p_1p_1'' - (p_1')^2). \end{cases} \tag{A9}$$

We have used the fact that

$$16q_c^4 D - 4q_c^2 P_c R = \tfrac{32}{3} q_c^4 D.$$

From (A8) we easily obtain

$$\begin{aligned} \hat{f}_0(x) &= 2q_c^2 R p_1(x)p_2(x) \\ \hat{w}_0(x) &= q_c^2 R p_1^2(x). \end{aligned} \tag{A10}$$

The problem (A9) must be solved with the appropriate boundary conditions that are deduced from eqns (5) or (6). Then we get the two coefficients α_{11} and α_{30} in (A1):

$$\begin{aligned} \alpha_{11} &= 2\frac{\mathrm{d}\mathscr{L}_2}{\mathrm{d}P}(u_1) = -R\int_{-L/2}^{L/2}\int_0^{2\pi R} (\partial_y w_1)^2 \,\mathrm{d}x\,\mathrm{d}y \\ &= -4q_c^2\pi R^2 \int_{-L/2}^{L/2} p_1^2 \,\mathrm{d}x \end{aligned} \tag{A11}$$

$$\begin{aligned} \alpha_{30} &= -4\mathscr{L}_2(\hat{\mathbf{v}}) = 2\mathscr{L}_{21}(\mathbf{u}_1, \hat{\mathbf{v}}) \\ &= -\int_{-L/2}^{L/2}\int_0^{2\pi R} (2[w_1, f_1]\hat{w} + [w_1, w_1]\hat{f}) \,\mathrm{d}x\,\mathrm{d}y. \end{aligned} \tag{A12}$$

If we introduce the following notation

$$\alpha_{30} = \alpha_{30}^0 + \alpha_{30}^2, \tag{A13}$$

we get

$$\alpha_{30}^0 = 4\pi R q_c^2 \int_{-L/2}^{L/2} \{2(p_1p_2)''\hat{w}_0 + (p_1^2)''\hat{f}_0\} \,\mathrm{d}x \tag{A14}$$

$$\alpha_{30}^2 = 4\pi R q_c^2 \int_{-L/2}^{L/2} \{(p_1''p_2 + p_1p_2'' - 2p_1'p_2')\hat{w}_2 + (p_1''p_1 - p_1'^2)\hat{f}_2\} \,\mathrm{d}x. \tag{A15}$$

By using (60b) and (A10), we obtain

$$\begin{aligned} \alpha_{30}^0 &= -8\pi REh \int_{-L/2}^{L/2} \{(p_1p_1'')''p_1^2 + (p_1^2)''p_1p_1''\} \,\mathrm{d}x \\ \alpha_{30}^2 &= -\frac{4\pi Eh}{q_c^2} \int_{-L/2}^{L/2} \{(((p_1'')^2 + p_1p_1'''' - 2p_1'p_1''')\hat{w}_2 + \tfrac{1}{16}(p_1''p_1 - p_1'^2)(\hat{w}_2'' - 2q_c^2 R(p_1p_1'' - (p_1')^2))\} \,\mathrm{d}x \end{aligned} \tag{A16}$$

where $\hat{w}_2(x)$ is solution of the following problem:

$$\hat{w}_2'''' + 4\sigma^4\left(\frac{\pi}{L}\right)^4 \hat{w}_2 = 2q_c^2 R(p_1p_1'' - (p_1')^2)'' + 32q_c^2 R\{(p_1'')^2 + p_1p_1'''' - 2p_1'p_1'''\} \tag{A17}$$

$$\sigma^4 = 2^7. \tag{A18}$$

The boundary conditions are:

1. In the case $N_x = 0$

$$\hat{w}_2\left(\pm\frac{L}{2}\right) = 0, \quad \hat{w}_2''\left(\pm\frac{L}{2}\right) = -2q_c^2 R\left(\frac{\pi}{L}\right)^2. \tag{A19}$$

2. In the case $u = 0$

$$\hat{w}_2\left(\pm\frac{L}{2}\right) = \hat{w}_2'\left(\pm\frac{L}{2}\right) = 0. \tag{A20}$$

Case without axial restraint

In this case we get from (60) and (61) the identity

$$\begin{cases} p_1 p_1'' - (p_1')^2 = -\frac{1}{4}\left(\frac{\pi}{L}\right)^2 \\ (p_1'')^2 + p_1 p_1'''' - 2p_1' p_1''' = \frac{1}{2}\left(\frac{\pi}{L}\right)^4. \end{cases} \tag{A21}$$

The problem (A17)–(A19) is then in the form

$$\begin{cases} \hat{w}_2'''' + 4\sigma^4\left(\frac{\pi}{L}\right)^4 \hat{w}_2 = 16 q_c^2 R\left(\frac{\pi}{L}\right)^4 \\ \hat{w}_2\left(\pm\frac{L}{2}\right) = 0, \quad \hat{w}_2''\left(\pm\frac{L}{2}\right) = -2q_c^2 R\left(\frac{\pi}{L}\right)^2. \end{cases} \tag{A22}$$

One gets the solution:

$$\hat{w}_2(x) = \frac{Rq^2}{2^5}\left\{1 + A\cosh\frac{\sigma\pi x}{L}\cos\frac{\sigma\pi x}{L} + B\sinh\frac{\sigma\pi x}{L}\sin\frac{\sigma\pi x}{L}\right\} \tag{A23}$$

where A and B are given by the boundary conditions. The result is

$$A = \frac{1/\sqrt{2}E - F}{E^2 + F^2} \tag{A24}$$

$$B = -\frac{1/\sqrt{2}F + E}{E^2 + F^2} \tag{A25}$$

$$E = \sinh(2^{3/4}\pi)\sin(2^{3/4}\pi) \tag{A26}$$

$$F = \cosh(2^{3/4}\pi)\cos(2^{3/4}\pi). \tag{A27}$$

Finally, we get after integration, the coefficients α_{11}, α_{30} and the factor b:

$$\begin{aligned} \alpha_{11} &= -\tfrac{1}{4}q_c^2\pi R^2 L \\ \alpha_{30} &= -2\pi^2 REh\left(\frac{\pi}{L}\right)^3 \times 0.2683 \\ b &= -\frac{\alpha_{30}}{\alpha_{11}} = -1.0732\frac{Eh}{q_c^2 R}\left(\frac{\pi}{L}\right)^4. \end{aligned} \tag{A28}$$

Case with an axial restraint

In this case we get from eqns (60) and (61) the identity

$$\begin{cases} p_1 p_1'' - (p_1')^2 = \left(\frac{r\pi}{L}\right)^2\left\{-\alpha^2 + \beta^2 + 2\alpha\beta\sin\frac{r\pi}{L}x\sinh\frac{r\pi}{L}x\right\} \\ (p_1'')^2 + p_1 p_1'''' - 2p_1' p_1''' = 2\left(\frac{r\pi}{L}\right)^4\{\alpha^2 + \beta^2\}. \end{cases} \tag{A29}$$

The problem (A17)–(A19) is then in the form:

$$\begin{cases} \hat{w}_2'''' + 4\sigma^4\left(\frac{r\pi}{L}\right)^4 \hat{w}_2 = 64 q_c^2 R\left(\frac{r\pi}{L}\right)^4\left\{\alpha^2 + \beta^2 + \frac{\alpha\beta}{8}\cos\frac{r\pi x}{L}\cosh\frac{r\pi x}{L}\right\} \\ \hat{w}_2\left(\pm\frac{L}{2}\right) = \hat{w}_2'\left(\pm\frac{L}{2}\right) = 0. \end{cases} \tag{A30}$$

One gets the solution:

$$\dot{w}_2(x) = q_c^2 \frac{R(\alpha^2+\beta^2)}{2^3}\left\{1 + A\cosh\frac{\sigma r\pi}{L}x\cos\frac{\sigma r\pi}{L}x + B\sinh\frac{\sigma r\pi}{L}x\sin\frac{\sigma r\pi}{L}x + \frac{16\alpha\beta}{(2^7-1)(\alpha^2+\beta^2)}\cos\frac{r\pi}{L}x\cosh\frac{r\pi}{L}x\right\} \tag{A31}$$

where A and B are given by the boundary conditions

$$\begin{cases} A = \dfrac{C1D4 - D2C2}{D1D4 - D2D3} \\ B = \dfrac{C2D1 - C1D3}{D1D4 - D2D3} \end{cases} \tag{A32}$$

$$C1 = \frac{2^4}{(1-2^7)}\frac{\alpha\beta}{\alpha^2+\beta^2}\cosh\frac{r\pi}{2}\cos\frac{r\pi}{2} - 1$$

$$C2 = \frac{2^{9/4}}{1-2^7}\frac{\alpha\beta}{\alpha^2+\beta^2}\left(\sinh\frac{r\pi}{2}\cos\frac{r\pi}{2} - \sin\frac{r\pi}{2}\cosh\frac{r\pi}{2}\right)$$

$$D1 = \cosh(2^{3/4}r\pi)\cos(2^{3/4}r\pi)$$

$$D2 = \sinh(2^{3/4}r\pi)\sin(2^{3/4}r\pi)$$

$$D3 = \sinh(2^{3/4}r\pi)\cos(2^{3/4}r\pi) - \cosh(2^{3/4}r\pi)\sin(2^{3/4}r\pi)$$

$$D4 = \sinh(2^{3/4}r\pi)\cos(2^{3/4}r\pi) + \cosh(2^{3/4}r\pi)\sin(2^{3/4}r\pi). \tag{A33}$$

Then after integration we get the coefficients α_{11}, α_{30} and the factor b:

$$\alpha_{11} = -0.3114 q_c^2 R^2 L$$

$$\alpha_{30} = -\tfrac{1}{2}\pi^2 REh\left(\frac{\pi}{L}\right)^3 \times 0.6868$$

$$b = -\frac{\alpha_{30}}{\alpha_{11}} = -3.4644\frac{Eh}{q_c^2 R}\left(\frac{\pi}{L}\right)^4. \tag{A34}$$